ACADEMIC PRESS

Available online at www.sciencedirect.com
SCIENCE DIRECT®

Journal of Catalysis 218 (2003) 386–395

JOURNAL OF CATALYSIS

www.elsevier.com/locate/jcat

NEXAFS spectroscopy study of the surface properties of zinc glutarate and its reactivity with carbon dioxide and propylene oxide

J.-S. Kim,[a] M. Ree,[a,*] S.W. Lee,[a] W. Oh,[a] S. Baek,[a] B. Lee,[a] T.J. Shin,[a] K.J. Kim,[b] B. Kim,[b] and J. Lüning [c]

[a] *Department of Chemistry, Center for Integrated Molecular Systems, BK21 Program, Division of Molecular and Life Sciences, and Polymer Research Institute, Pohang University of Science and Technology, San 31, Hyoja-dong, Pohang 790-784, Republic of Korea*

[b] *Pohang Accelerator Laboratory, Pohang University of Science and Technology, San 31, Hyoja-dong, Pohang 790-784, Republic of Korea*

[c] *Stanford Synchrotron Laboratory, MS 69, PO Box 20450, Stanford, CA 94209, USA*

Received 10 December 2002; revised 21 February 2003; accepted 10 March 2003

Abstract

The surface state of polycrystalline zinc glutarate (ZnGA) catalyst and its catalytic adsorption of carbon dioxide (CO_2) and propylene oxide (PO) were investigated by using near edge X-ray absorption fine structure (NEXAFS) spectroscopy. The outermost layer of ZnGA catalyst was found to contain more hydrocarbon units (i.e., glutarate ligand component) than the inner layers. The ZnGA catalyst was found to reversibly react with CO_2 and to readily react with PO via adsorption onto the catalyst surface and insertion into the Zn–O bond. Experiments in which the catalyst was treated with CO_2 followed by PO and vice versa showed that each of these components can replace the other component on the catalyst surface. This reversible adsorption and insertion of CO_2 and PO on the ZnGA surface provides a clue to the mechanism underlying the production of alternating poly(propylene carbonate) in the ZnGA-catalyzed copolymerization of CO_2 and PO. However, in comparison to CO_2, PO was more easily adsorbed onto the ZnGA catalyst and inserted into the Zn–O bond. As a consequence, PO significantly modified the catalyst surface. This suggests that the ZnGA-catalyzed copolymerization is initiated by PO rather than CO_2.

Keywords: Zinc glutarate catalyst; NEXAFS; Copolymerization of CO_2 with propylene oxide

1. Introduction

The copolymerization of CO_2 and oxirane is widely regarded as an effective method for CO_2 fixation. Importantly, the product of this reaction, polyalkylenecarbonate (PAC), has numerous potential applications in various areas of the polymer industry; for example, it could be used as a commodity polymer to replace some polyolefins, as a biomedical or environmental polymer due to its biocompatibility, and as a temporary disposable binder on account of its complete thermal decomposition properties. A variety of materials are known to catalyze the copolymerization of CO_2 and oxirane [1–14]. Among the catalysts considered to date, zinc dicarboxylates have proved to be among the most effective for producing reasonably high molecular weight PAC with high polymerization yield in the copolymerization [9–14]. In particular, zinc glutarate (ZnGA) was found to give the highest yield in the synthesis of PAC [9,13]. The low cost of the raw chemicals required to prepare ZnGA catalyst make this catalyst the most cost-effective catalyst for converting CO_2 resources into PAC materials that can be used in the polymer industry [9,12–14].

Most active ZnGA catalysts are generally prepared as powders from zinc oxide and glutaric acid [9,11]. The ZnGA catalyst is insoluble in solvents including water [9,11]. Only in highly acidic solutions (pH < 2), the catalyst dissolves via dissociation [9,11]; thus, the ZnGA acts as a heterogeneous rather than homogeneous catalyst in the copolymerizations. Due to this inherent insolubility, the single crystal formation of the ZnGA was not succeeded. Furthermore, the insolubility highly restricted studies of the structure and the catalytic activity of the ZnGA catalyst. Only structure and catalytic mechanisms of the heterogeneous catalyst ZnGA have been studied with a view to improving its catalytic activity and to developing new catalysts with higher catalytic activity [15–18]. To date, however, little is known about the

* Corresponding author.
E-mail address: ree@postech.edu (M. Ree).

0021-9517/03/$ – see front matter
doi:10.1016/S0021-9517(03)00122-2

surface state of ZnGA, which is usually a polycrystalline material, and the reactivity of ZnGA with CO_2 and oxirane monomers remains poorly understood.

In the present study, we investigated the surface characteristics of ZnGA catalyst and examined catalytic adsorptions of CO_2 and propylene oxide (PO) on the catalyst surface using carbon (C) *K*-edge and oxygen (O) *K*-edge near edge X-ray absorption fine structure (NEXAFS) spectroscopy. NEXAFS spectroscopy is a powerful tool for determining the local atomic structure and the electronic properties around the X-ray absorbing atoms in molecules, and in many cases this technique can even be used to examine disordered adsorption systems [19]. NEXAFS spectra with different surface sensitivities can be simultaneously measured by means of the Auger electron yield (AEY) and total electron yield (TEY) detection modes [22]. The AEY measurement uses an electron energy analyzer to monitor the intensity of elastically emitted Auger electrons. Sampling depth is given by the elastic mean free path of the Auger electrons in the material, which is for the C KVV Auger electrons in carboceous materials usually on the order of 1.5 nm. Hence, AEY measurements sample only the near subsurface region [20]. In TEY measurements, on the other hand, all of the electrons emitted from the sample surface (i.e., elastically scattered Auger and all other electrons) are counted. The TEY signal is dominated by the low energy electrons excited in the inelastic scattering cascade of the primary Auger electrons. Since these low kinetic energy electrons have undergone several scattering events, TEY probes deeper below the sample surface than does AEY [20]. In the present work, we use the unique capabilities of surface-sensitive NEXAFS spectroscopy to investigate the changes of chemical composition at the surface of a ZnGA catalyst resulting from the adsorption and reaction of CO_2 and PO.

2. Experimental

ZnGA catalyst was prepared from zinc oxide (ZnO) and glutaric acid (GA) as described elsewhere [9,11,12]. ZnGA samples for NEXAFS measurements were prepared by scrubbing a powder of the catalyst onto scratched silicon (Si) wafers. The resulting ZnGA-scrubbed Si wafers were treated with CO_2 or PO in one of four ways: (i) exposure to 100 or 300 psi CO_2 for 10 h in an autoclave, (ii) dipping in boiling PO for 30 or 60 min, (iii) exposure to 300 psi CO_2 for 10 h and subsequent dipping into boiling PO for 4 h, and (iv) dipping into boiling PO for 4 h and subsequent exposure to 300 psi CO_2 for 10 h. The size of each sample was 1×1 cm^2.

NEXAFS measurements were conducted at the NEXAFS beamline (BL 10-1) of Stanford Synchrotron Radiation Laboratory (Stanford, USA) and at the 2B1 VUV beamline of Pohang Accelerator Laboratory (Pohang, Korea) [21]. The photon energy resolution was about 100 meV around 300 eV. The spectra were divided by the total electron yield signal from a highly transmissive (about 80%) gold grid, measured with a picoammeter. A pre-edge background was then subtracted from the normalized spectra and the edge jump far above the *K*-edge (340–380 eV for C *K*-edge; 570–590 eV for O *K*-edge) was arbitrarily scaled to unity. This procedure produces NEXAFS spectra in which all resonance intensities correspond to the same number of C or O atoms in the sample, as discussed elsewhere [22]. The energy scale was calibrated using the carbon-induced structure at 284.7 eV in the monochromator transmission function. The reproducibility of the measured spectra was carefully checked by comparing multiple scans. No evidence of beam damage was found. Spectra measured with an X-ray spot size of 0.1×1 mm^2 did not change with time. The specimen was mounted on a rotatable holder that made it possible to rotate the specimen around a vertical axis to change the incidence angle θ of the X-ray beam relative to the specimen surface. However, as expected for a polycrystalline sample the spectra reported here do not show any dependence on the angle between the beam and the ZnGA sample; hence, all spectra were recorded at a fixed incident angle of 55°.

NEXAFS measurements were additionally conducted on ZnGA-scrubbed Si wafers exposed to CO_2 in the following way. Each sample was first mounted on a holder equipped with a tungsten-wire heater and moved into the second vacuum chamber of the sample compartment at the NEXAFS beamline. The sample was then annealed at about 70 °C under high vacuum (10^{-9} Torr) for 2 h, after which it was exposed to by injecting into the second chamber. The exposure was 600 or 1200 Langmuir (L) (1 L $= 10^{-6}$ Torr/s) at 7×10^{-6} Torr. Within 10 min of the exposure, the sample was moved into the first vacuum chamber at 10^{-9} Torr and the NEXAFS measurements were carried out. The cycle of exposure and NEXAFS measurement was repeated at least two times for each sample.

In addition, X-ray photoelectron spectroscopy (XPS) measurements were carried out to determine the surface composition of the ZnGA catalyst using a PHI 5400ESCA system with a Mg-K_α 350 W X-ray source. The vacuum level in the sample chamber was maintained at 2.0×10^{-9} Torr. The binding energies were calibrated with respect to the signal for adventitious carbon (binding energy = 284.6 eV).

3. Results and discussion

3.1. C *K*-edge and O *K*-edge NEXAFS spectra

Fig. 1 displays NEXAFS spectra measured from the ZnGA catalyst before and after annealing at 70 °C. In the ZnGA catalyst, Zn metal ions are coordinated with glutarate (GA) ligands composed of two carboxyl end groups and three methylene units. The C *K*-edge and O *K*-edge NEXAFS spectra originating from the GA ligand have been assigned with the aid of NEXAFS results previously reported

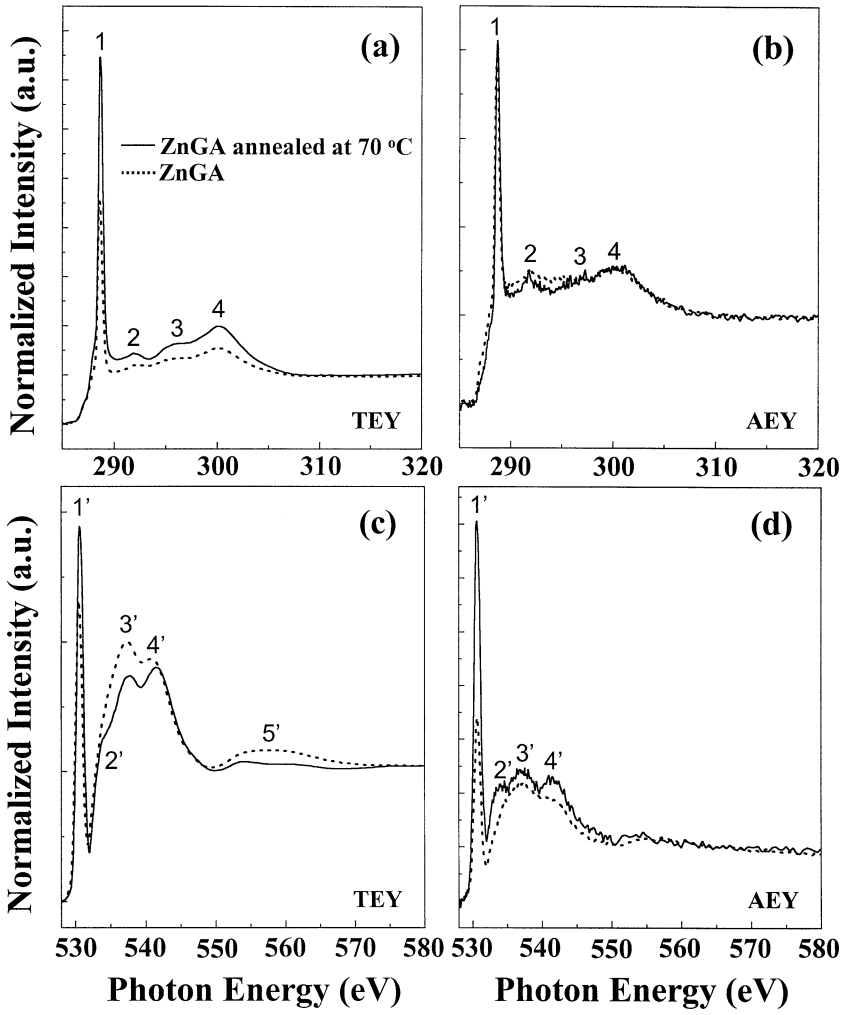

Fig. 1. C and O K-edge near edge X-ray absorption fine structure (NEXAFS) spectra measured from zinc glutarate (ZnGA) before and after annealing at 70 °C. NEXAFS spectra were measured in total electron yield (TEY) at (a) C K-edge and (c) O K-edge and Auger electron yield (AEY) modes at (b) C K-edge and (d) O K-edge.

Table 1
Energies and tentative assignments of all major resonance peaks of zinc glutarate (ZnGA) measured by C and O K-edge near edge X-ray absorption fine structure spectroscopy

Resonance peak	Energy (eV) (C K-edge)	Assignment	Resonance peak	Energy (eV) (O K-edge)	Assignment
1	288.6	$\pi^*_{C=O}$	**1′**	530.5	$\pi^*_{C=O}$
2	291.9	σ^*_{C-C}	**2′**	534.1	$\pi^*_{C=O}$
3	296.3	σ^*_{C-O}, $\sigma^*_{C=O}$	**3′**	537.3	σ^*_{C-O}, $\sigma^*_{C=O}$
4	300.2	$\sigma^*_{C=O}$	**4′**	540.8	$\sigma^*_{C=O}$
			5′	557.5	σ^*_{C-O}

for compounds containing carboxyl and methylene units, specifically, saturated carboxylic acids [23], polymethylmethacrylate (PMMA) [22], and poly(ethylene terephthalate) (PET) [24–26]. The energies and assignments of the peaks in the NEXAFS spectra are summarized in Table 1.

As seen in Fig. 1a, a pronounced sharp peak **1** appears at 288.6 eV, which is attributed to the excitation of a C 1s electron of the carboxyl group to the empty π^* orbital. A weak shoulder peak is also observed at the low energy region of peak **1**, which may originate from C–H* resonance [27]. Other peaks appear at 296.3 eV and 300.2 eV (peaks **3** and **4**, respectively). These resonance energies are close to the characteristic resonance energies of the σ^* resonances of C–O and C=O in carboxyl group, respectively [28]. Thus, one might be tempted to assign peak **3** to the C–O σ^* resonance and peak **4** to the C=O σ^* resonance. However, our recent X-ray absorption near-edge structure (XANES) and extended X-ray absorption fine structure (EXAFS) spectroscopy studies at the Zn K-edge indicate that in the ZnGA catalyst the two oxygen atoms of each carboxyl end group of the GA ligand equally coordinate to the Zn metal atoms, making a tetrahedral coordinated complex with a Zn–O bond distance of 1.95–1.96 Å [18]. In this tetrahedral complex, the two oxygen atoms of each carboxyl end group of the GA ligand were found to coordinate to the Zn atoms in two different ways, *syn–syn* and *syn–anti* bridge configurations [18]. The presence of these two bridge structures was also evident in infrared spectroscopy results reported

elsewhere [10]. The tendency to form two bridge structures implies that the π-bonding character of the carbonyl bond in the carboxyl group of the GA ligand is rather delocalized to the adjacent C–O bond. Taking this structural information into account, peaks **3** and **4** may in fact arise mainly from the splitting of the delocalized C=O bond caused by σ^* bond-to-bond interactions [22]. While, the absorption peak **2** corresponds to the C–C σ^* resonance [23]. Taking into account the interactions of the adjacent σ^* bonds, peaks **3** and **4** are further affected by the σ^* splittings of the hydrocarbon and carboxyl group in the ZnGA. The effect of the σ^* splitting caused by the hydrocarbon may, however, be small due to the short alkylene length in the GA ligand. Collectively, the results lead to the conclusion that each carboxyl group of the Zn-coordinated GA ligand is in a degenerate state, and that the two bonds of the carboxyl group in the degenerate state interact with each other, causing splitting of the σ^* resonance. This interaction effect must be significant, given that the ZnGA catalyst has a network structure in which each Zn metal ion is tetrahedrally coordinated to four carboxyl oxygen atoms.

In the NEXAFS spectrum recorded in the AEY detection mode (Fig. 1b), peak **2** appears with relatively high intensity. Generally, NEXAFS spectroscopy in the AEY mode is sensitive to the chemical composition at the surface [29]. Thus, the appearance of such a strong peak **2**, which corresponds to the C–C σ^* resonance, indicates that the surface of the ZnGA catalyst is enriched with hydrocarbon units. This is supported by analysis of the XPS spectrum of the ZnGA catalyst, which shows that the concentration of carbon is higher than that predicted for a perfect ZnGA crystal and that the concentration of oxygen is lower than that of the ZnGA crystal (see Table 2). Furthermore, on the basis of the XPS results the coordination number of the zinc metal ions at the catalyst surface can be estimated to be 2.7. This coordination number is much lower than 4.0–4.3 determined previously by EXAFS analysis of the bulk ZnGA catalyst [18]. Taken together, the XPS and NEXAFS results indicate that unsaturated zinc metal ions are present on the outermost surface of the ZnGA catalyst.

Figs. 1c and 1d display the O *K*-edge NEXAFS spectra obtained from the ZnGA. The present oxygen content in the ZnGA gives good statistics of spectrum and useful information of coordination change between the zinc metal ion and the carboxyl groups of GA ligand. Adopting the NEXAFS results for PET and its analogues with carboxyl groups in the literature [24–26,30], the O *K*-edge NEXAFS spectral peaks are assigned as follows. The intense feature at 530.5 eV (peak **1**′), is assigned to the C=O π^* resonance, peak **3**′ at 537.3 eV is assigned to the C–O σ^* resonance, and peak **4**′ at 540.8 eV is assigned to the C=O σ^* resonance. However, as discussed above in relation to the C *K*-edge NEXAFS spectra, peak **3**′ may arise mainly from the splitting of C=O σ^* resonance due to the interaction of two C=O bonds in the degenerate state. Additional evidence for this degenerate state of the carboxyl group in the GA ligand is provided by the observation of a single O 1*s* peak without any shoulders in the XPS spectrum (see Fig. 2); the appearance of a single O 1*s* peak indicates that the oxygens in the carboxyl group are in almost the same state.

Table 2
A comparison of the theoretical (crystal) composition of zinc glutarate (ZnGA) with the composition as determined by X-ray photoemission spectroscopy (XPS)

XPS element	Area (cts-eV/s)	Sensitivity factor	Concentration (mol%)	Theoretical value (mol%)
Zn $2p_{3/2}$	116,814	3.726	8.28	10
O 1*s*	42,690	0.711	22.4	40
C 1*s*	54,071	0.296	69.32	50

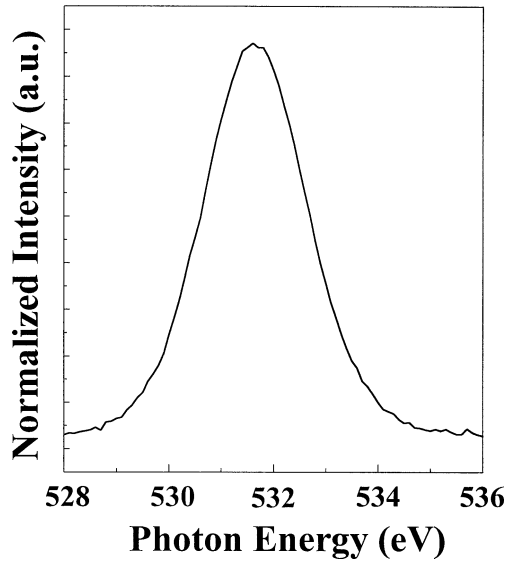

Fig. 2. O 1*s* absorption spectrum of ZnGA catalyst measured by X-ray photoemission spectroscopy.

We now consider the effects of structural defects in the ZnGA catalyst on the NEXAFS spectra, in particular the effects on peaks **3** and **4** in Figs. 1a and 1b as well as peaks **3**′ and **4**′ in Figs. 1c and 1d. The ZnGA used in this study was not a single crystal but rather a powder comprised of particles of high crystallinity [9]. Hence, the ZnGA catalyst possibly has defect sites originating from the presence of uncoordinated carboxyl end groups of the GA ligands or uncoordinated Zn metal ions, although the number of such sites is very small relative to the number of fully coordinated sites. In fact, the C–O single bond character indicating the presence of uncoordinated carboxyl groups is derived from the relatively weak intensity of the peak **3**′, compared to that of the peak **1**′, which is attributed to the weak contribution of the C–O σ^* resonance. Taking this result and any possible structural defects into account, we believe that peak **3** in the C *K*-edge spectrum and peak **3**′ in the O *K*-edge spectrum originate mainly from the splitting of the delocalized carboxyl σ^* resonances and *partially* from the C–O σ^* resonance.

3.2. Annealing effect on the ZnGA surface

The intensities of the NEXAFS spectra of the ZnGA catalyst vary after annealing of the catalyst at 70 °C under high vacuum. Overall, the C *K*-edge spectrum measured in the TEY mode (Fig. 1a) strengthens due to annealing. In contrast, the spectrum measured in the AEY mode does not show any intensity change with annealing (Fig. 1b).

Fig. 1c displays the O *K*-edge spectra of the ZnGA catalyst measured in the TEY mode before and after annealing. It is evident that annealing changes the intensities of the absorption peaks. Overall, annealing strengthens absorption peak **1**′ but weakens all other peaks. In particular, absorption peak **5**′ disappears almost completely after annealing. In contrast, a new absorption peak **2**′ at 534.1 eV is clearly discernible after annealing. The appearance of this new peak is accompanied by a strengthening of peak **1**′, which corresponds to the C=O π^* resonance. This suggests that peak **2**′ may be related to the C=O π^* resonance.

The effect of annealing on the absorption peaks is also clearly observed in the NEXAFS spectra measured in the AEY mode. As seen in Fig. 1d, all of the peaks are more intense after annealing. In particular, peak **2**′ is more distinct after annealing. However, the absorption peak **5**′ that is clearly detected in the TEY mode is barely distinguishable in the spectrum measured in the AEY mode due to the relatively large noise level.

The changes in the NEXAFS spectra caused by annealing may be directly related to interaction between the ZnGA catalyst and atmospheric CO_2. This point is discussed in detail in the following sections.

3.2.1. In situ CO_2 treatment of ZnGA

Some ZnGA catalyst specimens were first annealed at 70 °C and then treated with 600 or 1200 L CO_2, after which they were immediately characterized by NEXAFS spectroscopy. The resulting NEXAFS spectra are displayed in Fig. 3.

In the NEXAFS spectra of the ZnGA recorded in the TEY mode (Fig. 3a), all of the C *K*-edge absorption peaks are apparently suppressed by CO_2 treatment. Thereafter, the suppressed peaks are not changed with further varying CO_2

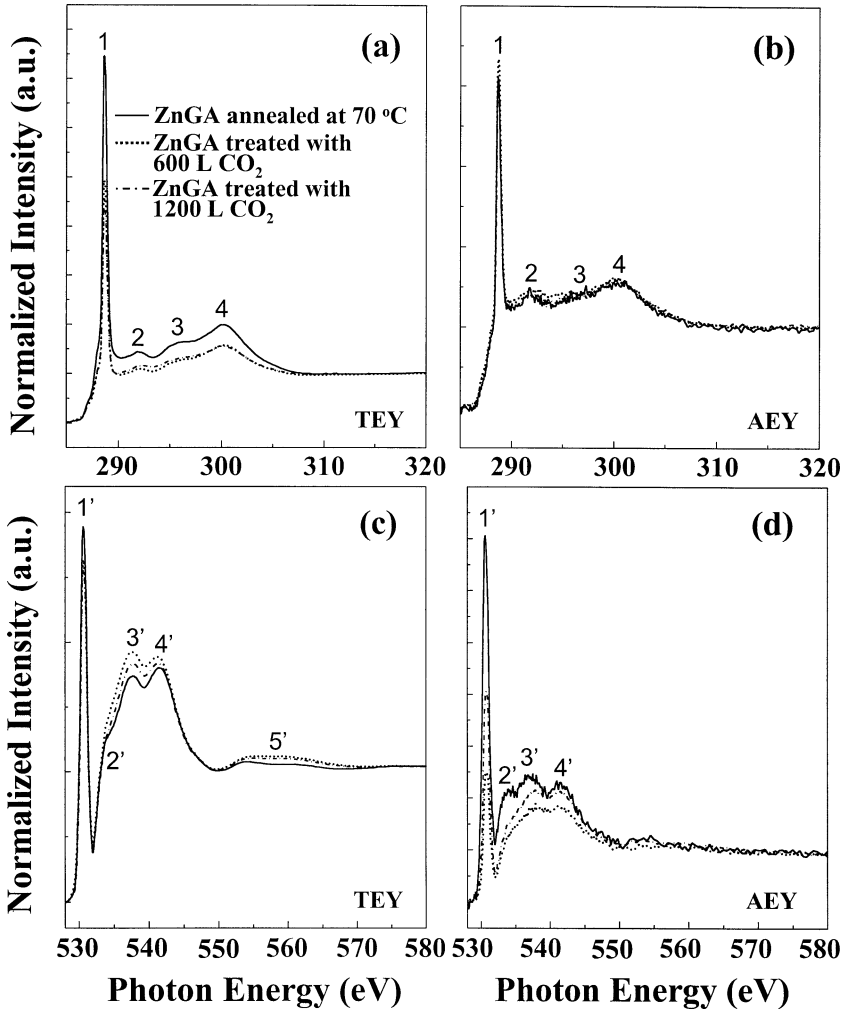

Fig. 3. C and O *K*-edge NEXAFS spectra of ZnGA catalysts annealed at 70 °C and in-situ treated with 600 to 1200 L CO_2. Spectra were measured in total electron yield (TEY) at (a) C *K*-edge and (c) O *K*-edge and Auger electron yield (AEY) modes at (b) C *K*-edge and (d) O *K*-edge.

dose. When peaks **2**, **3**, and **4** are normalized by the intensity of peak **1**, all the normalized peaks, however, show only slight changes due to the CO_2 treatments. The NEXAFS spectrum recorded in the AEY mode (Fig. 3b) shows very little variation after CO_2 treatment, regardless of the CO_2 dose. These results suggest that the carbon atoms of the GA ligand in the ZnGA are not involved in the reaction (or interaction) of ZnGA and CO_2.

In contrast to the C K-edge spectra, the O K-edge absorption spectrum is sensitive to CO_2 treatment. Comparison of the spectra measured in the TEY mode (Fig. 3c) before and after CO_2 treatment shows that treatment with CO_2 leads to a slight suppression of peak **1′**, and a strengthening of peaks **2′**, **3′**, **4′**, and **5′**. In the spectra measured in the AEY mode (Fig. 3d), peak **1′** is suppressed by CO_2 treatment to a much greater extent than it is in the TEY measurements. The other peaks (**2′**, **3′**, and **4′**) are also suppressed as a result of CO_2 treatment, although only to a small extent. All of the changes observed in the O K-edge spectra indicate that CO_2 reacts with the ZnGA catalyst, influencing the characteristics of the coordinated bonding between the Zn metal ion and the carboxyl group of the GA ligand.

Of particular importance is the CO_2-induced evolution of a peak centered at 557.5 eV (peak **5′**), which is in good agreement with the energy of the C–O σ^* resonance in cadmium carbonate ($CdCO_3$) [22]. Thus, peak **5′** is tentatively assigned to the σ^* resonance of the C–O bond formed by CO_2 insertion into the bond between Zn metal ion and the carboxyl group of the GA ligand. In addition, exposure of ZnGA to CO_2 causes a much greater change in peak **3′** than in peak **4′**. As mentioned earlier, peak **3′** originates mainly from the splitting of the delocalized carboxyl σ^* resonances of the carboxyl group of the GA ligand and partly from the σ^* resonance of the C–O single bond characteristic of the carboxyl group of the GA ligand. Taking this into account, the large variation in peak **3′** due to CO_2 treatment is attributed to an increase in the C–O single bond population as a result of CO_2 insertion into the coordination bond between the Zn metal ion and the carboxyl group of the GA ligand.

Various examples of CO_2 insertion into metal-oxygen bonds [M–OR (R: alkyl or aryl)] have been reported [31–33]. In particular, Kato et al. [33] found that the insertion reaction of CO_2 into Zn–OR complex (R: alkyl or aryl) is facile in a study using infrared and nuclear magnetic resonance spectroscopy. Their results, combined with the results of the present study, lead us to conclude that the changes in the O K-edge spectrum resulting from CO_2 treatment are due to the formation of a carbonate bond. The carbonate bond formation is discussed in more detail as follows.

When the insertion reaction of CO_2 into the Zn–O bond in the ZnGA catalyst takes place, possible coordination geometries about the central Zn ion are bidentate (**I**), bridge (**II**), and unidentate coordination (**III**):

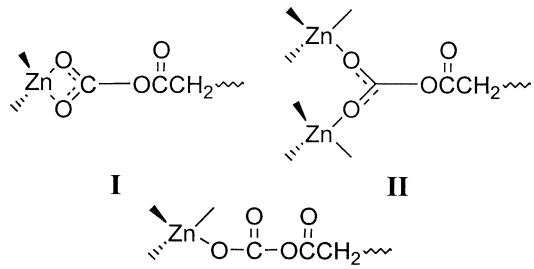

I **II**

III

where Zn is the zinc metal ion and –$OCOCH_2$∼ is the GA ligand.

Structures **I** and **II** contain only one C–O single bond, that of the carboxyl unit of the GA ligand. In contrast, structure **III** has two C–O single bonds, that of the carboxyl unit of the GA ligand and that of the oxygen involved in the unidentate coordination. All of the three possible coordinations due to the CO_2 insertion would positively contribute to the absorption peaks **3′** and **5′**, although structure **III** would contribute to these peaks to a greater extent than structures **I** and **II**.

Furthermore, in the cases of the structures **I** and **II**, we must also consider the effect of the extra molecular interaction to the unoccupied π^* orbital. It is well known that K-shell excitation spectra are sensitive to extra molecular interactions (i.e., charge transfer) [34]. The $1s \rightarrow \pi^*$ energies and particularly the transition intensities, which are directly related to the C_{2p} and O_{2p} contributions to the π^* orbital, can be used to probe charge transfer in metal–ligand complexes. Blyholder [35] first suggested that charge transfer from the metal $d\pi$ orbital to the absorbate $2p$ orbital strengthens the metal-adsorbate bond but weakens the intramolecular bond [36]. The softening of the intramolecular bond on the ligand usually leads to a reduction in vibrational frequency. With increasing bond strength, the metal $d\pi-p\pi$ orbitals with the $2\pi^*$ orbital increase and the π^* resonance intensity decreases [22]. Therefore, when the CO_2 insertion take place via bidentate or bridge coordination, the intensity of the $1s \rightarrow \pi^*$ resonance may decrease due to charge transfer between the Zn metal and carbonyl oxygen. The coordination is generally known to significantly influence the peak intensities of $1s \rightarrow \pi^*$ transitions but not to affect their energies [22]. Comparison of the NEXAFS spectra of ZnGA catalysts before and after treatment with CO_2 shows just such an intensity reduction in the $1s \rightarrow \pi^*$ resonance (peak **1′** in Figs. 3c and 3d). This suggests that a bidentate and/or bridge coordination forms during CO_2 insertion into ZnGA. The reduction in the intensity of peak **1′** is much larger in the AEY mode than in the TEY mode, indicating that CO_2 insertion into ZnGA through the bidentate and/or bridge coordination occurs more favorably at the outermost surface layer rather than in an inner layer (i.e., a bulk layer). This is logical given that the outermost layer, which has sites with

uncoordinated Zn metal ions, has a greater chance than the inner layers of coming into contact with CO_2 molecules.

The NEXAFS spectra of ZnGA catalysts treated with CO_2 after annealing are almost identical to those of unannealed ZnGA catalyst which was already exposed to CO_2 in air through its handling. This result indicates two things. First, the CO_2 amount and subsequently inserted into the ZnGA catalyst sample is supplied sufficiently by the CO_2 concentration naturally present in air; namely, the CO_2 adsorption level of ZnGA catalyst might be small. Second, CO_2 adsorbed and inserted into the ZnGA catalyst is removed reversibly by thermal annealing. Similar reversible CO_2 insertion behavior has been observed in other organometallic compounds [37].

3.2.2. ZnGA treated with high pressure CO_2

Fig. 4 shows the O *K*-edge NEXAFS spectra acquired after ZnGA catalysts has been treated with 300 or 700 psi CO_2 for 10 h. These CO_2 pressures are typical conditions used in the copolymerization of CO_2 with oxirane, which gives a high PAC product yield [9]. Surprisingly, the NEXAFS spectrum of the ZnGA catalyst changed very little after exposure to high pressure CO_2, as can be seen in Fig. 4. In fact, as discussed above, the ZnGA catalyst had already been exposed to atmospheric CO_2 through its handling in the experiment. The NEXAFS results therefore suggest that the very limited amount of atmospheric CO_2 to which the catalyst was exposed during handling was sufficient to use up all of the reactive capacity of the catalyst. Thus, the ZnGA catalyst either has only limited reactivity with CO_2 or has only a limited number of reactive sites for CO_2. This low reactivity may originate from the weak basicity of the oxygen of the stable CO_2, compared to the oxygen of oxirane. Moreover, the low reactivity suggests that the ZnGA-catalyzed copolymerization of CO_2 with oxirane is not initiated by CO_2.

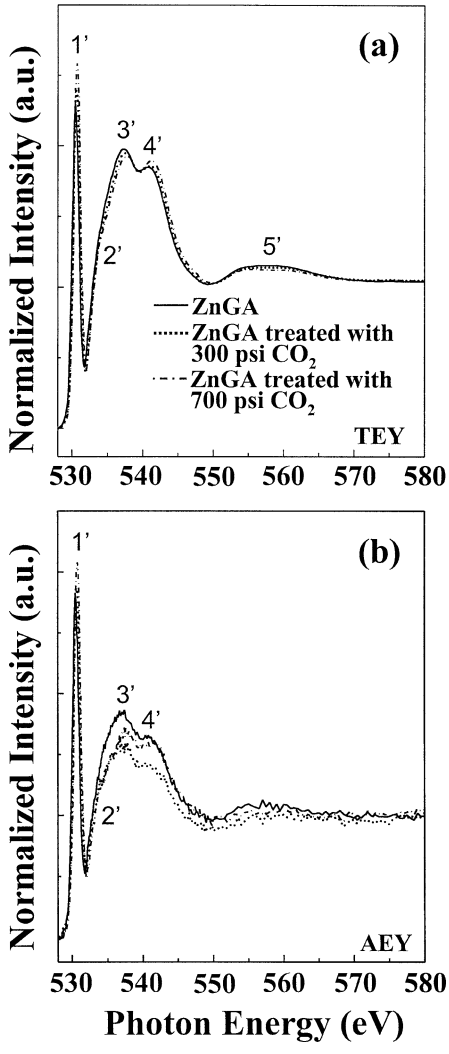

Fig. 4. O *K*-edge NEXAFS spectra of ZnGA catalyst before and after treatment with 300 to 700 psi CO_2. Spectra were measured in (a) total electron yield (TEY) and (b) Auger electron yield (AEY) modes.

3.3. ZnGA treated with boiling PO

Fig. 5 shows the C and O *K*-edge NEXAFS spectra acquired after ZnGA had been dipped into boiling PO for 30 to 60 min. As seen in Fig. 5a, the PO treatment significantly weakened all of the peaks in the C *K*-edge NEXAFS spectra measured in the TEY mode. In particular, peaks **1** and **4** in both the TEY and AEY mode spectra were severely weakened by the PO treatments (see Figs. 5a and 5b). These changes in peak intensity may originate from the adsorption of PO molecules onto the ZnGA surface and/or reaction of PO molecules with the ZnGA surface. Contrary to the general trend, the PO treatments caused an enhancement of the shoulder peak of resonance peak **1**, which corresponds to the C–H* resonance, in both the TEY and AEY modes. This peak enhancement might also be attributed to the methyl and methylene units of PO molecules adsorbed onto or/and reacted with ZnGA surface.

In the O *K*-edge NEXAFS spectrum, on the other hand, the PO treatments caused a significant strengthening of peaks **3′**, **4′**, and **5′** and a weakening of peak **1′** (Fig. 5c). In particular, the strengthening of peak **3′** is much stronger than that of peak **4′**. As discussed earlier, peak **3′** originates in part from the C–O σ^* resonance and peak **5′** originates from the C–O σ^* resonance. Thus, the observation of a strong PO-induced enhancement of peaks **3′** and **5′** is evidence that the PO molecule is inserted into the Zn metal ion and carboxyl group of the GA ligand, forming the following coordination structure with C–O bond characteristics (**IV**):

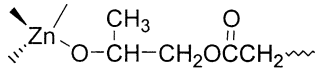

IV

In particular, the strengthening of peak **3′** as a result of the PO treatments is much stronger than that resulting from the CO_2 treatments. This suggests that the ZnGA-catalyzed copolymerization of CO_2 with PO is initiated by the PO

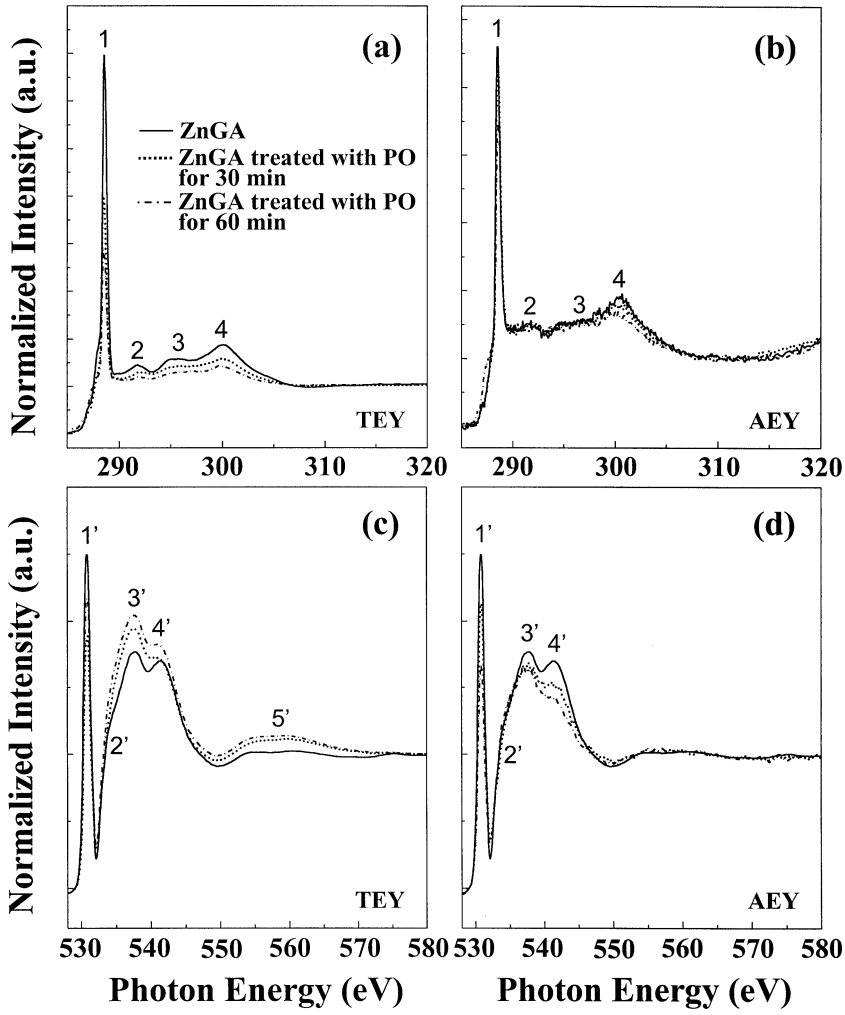

Fig. 5. C and O K-edge NEXAFS spectra of ZnGA catalyst before and after dipping in boiling PO for 30 to 60 min. Spectra were measured in total electron yield (TEY) at (a) C K-edge and (c) O K-edge and Auger electron yield (AEY) modes at (b) C K-edge and (d) O K-edge.

monomer, which is more easily adsorbed onto the ZnGA surface and is inserted into the Zn–O bond of the catalyst.

3.4. ZnGA treated with PO and CO_2

Fig. 6 shows the C and O K-edge NEXAFS spectra acquired after ZnGA had been treated with CO_2 and then PO or vice versa. When ZnGA was treated with CO_2 followed by PO, the C K-edge NEXAFS spectrum of the treated catalyst (Fig. 6a) was similar to that of the catalyst treated with PO alone, both in terms of relative intensity and shape. The spectra do show, however, some differences. Peaks **1** and **2** for the catalyst treated with CO_2 followed by treatment with PO for 4 h are more blurred than those of the catalyst treated with only PO for 1 h. This could be due to the different durations of the PO treatment. In addition, peak **3′** in the O K-edge NEXAFS spectrum is much stronger than that of the catalyst treated with PO alone. However, when the order of treatment is reversed such that the catalyst is treated with PO first and then with CO_2, the resulting C and O K-edge NEXAFS spectra are similar to those of the catalyst treated with CO_2 alone. In summary, these results suggest that the surface state of ZnGA is the state induced by the final treating species (i.e., CO_2 or PO), which indicates that the reaction of the initial species with the catalyst surface is reversible. This reversibility of the ZnGA surface state in the interactions with CO_2 and PO is directly related to the production of alternating poly(propylene carbonate) from the copolymerization of CO_2 and PO that occurs with the aid of the ZnGA catalyst [9].

4. Conclusions

The surface state of polycrystalline ZnGA catalyst and its catalytic adsorption of CO_2 and PO were studied in detail using C and O K-edge NEXAFS spectroscopy. The outermost layer of the ZnGA catalyst was found to contain more hydrocarbon units than the inner layers. Adsorption of CO_2 and PO onto the ZnGA catalyst and insertion of these molecules into the Zn–O bond of the catalyst were detected. However, the adsorbed and inserted into the ZnGA

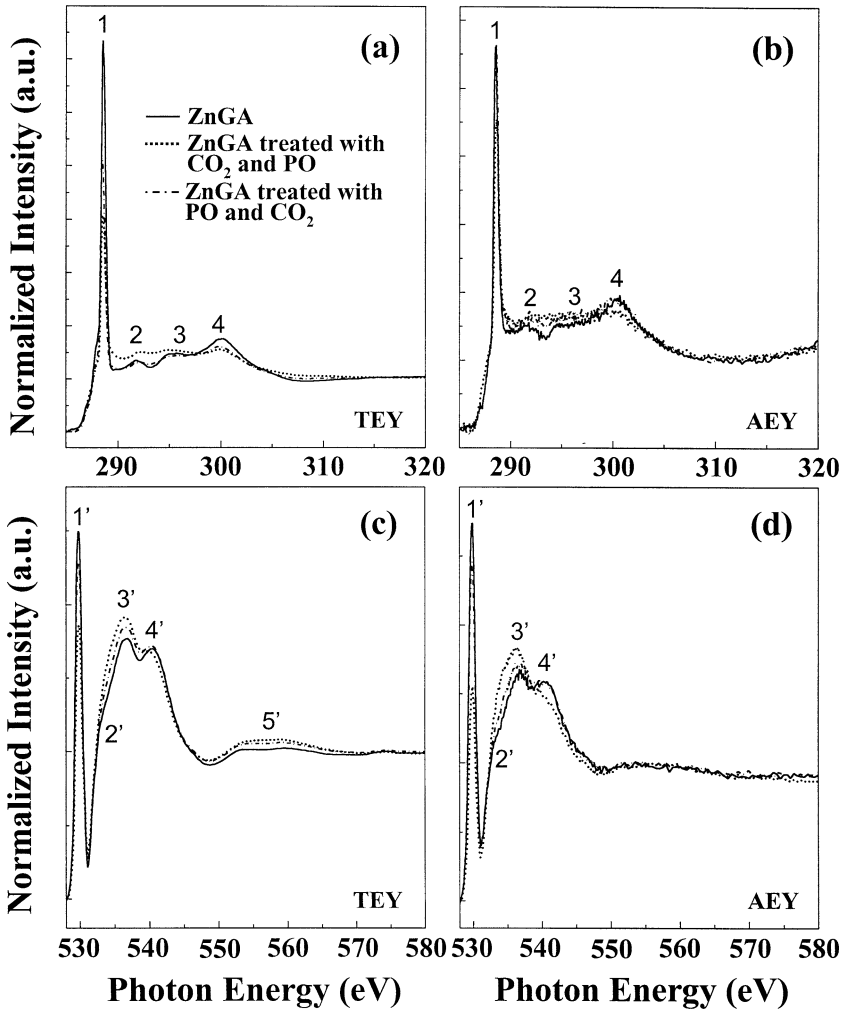

Fig. 6. C and O *K*-edge NEXAFS spectra of ZnGA catalyst before and after treatment with CO_2 and PO. Spectra were measured in total electron yield (TEY) at (a) C *K*-edge and (c) O *K*-edge and Auger electron yield (AEY) modes at (b) C *K*-edge and (d) O *K*-edge.

catalyst was replaced by PO treatment and vice versa, indicating that the surface state of ZnGA is changed reversibly by the final treating species (i.e., CO_2 or PO). This reversible adsorption and insertion of CO_2 and PO onto the ZnGA surface provides a clue to the mechanism by which alternating poly(propylene carbonate) is produced in the ZnGA-catalyzed copolymerization of CO_2 and PO. However, in comparison to CO_2, PO was more easily adsorbed onto the ZnGA catalyst and inserted into the Zn–O bond. As a consequence, PO significantly modified the catalyst surface. This suggests that the ZnGA-catalyzed copolymerization is initiated by PO rather than CO_2.

Acknowledgments

This study was supported by the Center for Integrated Molecular Systems (KOSEF) and by the Ministry of Education (BK21 Program). The NEXAFS measurements at Pohang Accelerator Laboratory were supported by POSCO and the Korean Ministry of Science and Technology. The NEXAFS measurements were carried out at the Stanford Synchrotron Radiation Laboratory, a national user facility operated by Stanford University on behalf of the US Department of Energy, Office of Basic Energy Sciences.

References

[1] (a) S. Inoue, H. Koinuma, T. Tsuruta, J. Polym. Sci. Polym. Lett. Ed. 7 (1969) 287;
(b) S. Inoue, H. Koinuma, T. Tsuruta, Macromol. Chem. 130 (1969) 210.
[2] A. Rokicki, W. Kuran, Macromol. Chem. 177 (1979) 135.
[3] K. Soga, E. Imai, I. Hattori, Polym. J. 13 (1981) 407.
[4] D.J. Darensbourg, M.W. Holtcamp, Coord. Chem. Rev. 53 (1996) 155.
[5] C.-S. Tan, T.-J. Hsu, Macromolecules 30 (1997) 3147.
[6] M. Cheng, E. Lobkovsky, G. Coates, J. Am. Chem. Soc. 120 (1998) 11018.
[7] D.J. Darensbourg, J. Wildeson, J. Yarbrough, J. Reibenspies, J. Am. Chem. Soc. 122 (2000) 12487.
[8] D.J. Darensbourg, M.W. Holtcamp, G.E. Struck, M.S. Zimmer, S.A. Niezgoda, P. Rainey, J.B. Robertson, J.D. Draper, J.H. Reibenspies, J. Am. Chem. Soc. 121 (1991) 107.
[9] M. Ree, J.Y. Bae, J.H. Jung, T.J. Shin, J. Polym. Sci: Part A: Polym. Chem. 37 (1999) 1863.

[10] M. Ree, J.Y. Bae, J.H. Jung, T.J. Shin, Y.T. Hwang, T. Chang, Polym. Eng. Sci. 40 (1991) 1542.
[11] M. Ree, J.Y. Bae, J.H. Jung, T.J. Shin, Kor. Polym. J. 7 (1999) 333.
[12] S.A. Motika, T.L. Pickering, A. Rokicki, B.K. Stein, US Patent 5,026,676, June 25, 1991.
[13] Y.Z. Meng, L.C. Du, S.C. Tiong, Q. Zhu, A.S. Hay, J. Polym. Sci: Part A: Polym. Chem. 40 (2002) 3579.
[14] M.H. Chisholm, D. Navarro-Llobet, Z. Zhou, Macromolecules 35 (2002) 6494.
[15] D.J. Darensbourg, S.A. Niezgoda, M.W. Holtcamp, J.D. Draper, J.H. Reibenspies, Inorg. Chem. 36 (1997) 2426.
[16] D.J. Darensbourg, S.A. Niezgoda, M.W. Holtcamp, J.H. Reibenspies, Polyhedron 15 (1996) 2341.
[17] D.J. Darensbourg, M.S. Zimmer, Macromolecules 32 (1999) 2137.
[18] J.S. Kim., M. Ree, T.J. Shin, O.H. Han, S.J. Cho, Y.-T. Hwang, J.Y. Bae, J.M. Lee, R. Ryoo, J. Catalysis, in press.
[19] A. Imanishi, K. Isawa, F. Matsui, T. Tsuduki, T. Yokoyama, H. Kondoh, Y. Kitajima, T. Ohta, Surface Sci. 407 (1998) 282.
[20] J. Lüning, D.Y. Yoon, J. Stöhr, J. Electron Spectrosc. Relat. Phenom. 121 (2001) 265.
[21] S.-Y. Rah, T.-H. Kang, Y. Chung, B. Kim, K.-B. Lee, Rev. Sci. Instrum. 66 (1995) 1751.
[22] J. Stöhr, NEXAFS Spectroscopy, in: Springer Series in Sciences, Vol. 25, Springer, Heidelberg, 1992.
[23] D.A. Outka, J. Stohr, J.P. Rabe, J.D. Swalen, J. Chem. Phys. 88 (1988) 4076.
[24] T. Okajima, K. Teramoto, R. Mitsumoto, H. Oji, Y. Yamamoto, I. Mori, H. Ishii, Y. Ouchi, K. Seki, J. Phys. Chem. A 102 (1998) 7093.
[25] I. Koprinarov, A. Lippitz, J.F. Friedrich, W.E.S. Unger, Ch. Woll, Polymer 39 (1998) 3001.
[26] A.P. Hitchcock, S.G. Urquhart, E.G. Rightor, J. Phys. Chem. 96 (1992) 8736.
[27] J. Kikuma, B.P. Tonner, J. Electron Spectrosc. Relat. Phenom. 82 (1996) 53.
[28] Th. Gross, A. Lippitz, W.E.S. Unger, Appl. Surf. Sci. 68 (1993) 291.
[29] S.G. Urquhart, A.P. Hitchcock, A.P. Smith, H.W. Ade, W. Lidy, E.G. Rightor, G.E. Mitchell, J. Electron Spectrosc. Relat. Phenom. 100 (1999) 119.
[30] L.G.M. Pettersson, H. Agren, B.L. Schurmann, A. Lippitz, W.E.S. Unger, Int. J. Quantum Chem. 63 (1997) 749.
[31] A.J. Goodsel, G. Blyholder, J. Am. Chem. Soc. 94 (1972) 6725.
[32] M.H. Chisholm, F.A. Cotton, M.W. Extine, W.W. Reichert, J. Am. Chem. Soc. 100 (1978) 1727.
[33] M. Kato, T. Ito, Inorg. Chem. 24 (1985) 504.
[34] E. Rühl, A.P. Hitchcock, J. Am. Chem. Soc. 111 (1989) 2614.
[35] G. Blyholder, J. Phys. Chem. 68 (1964) 2772.
[36] J. Stöhr, R. Jaeger, Phys. Rev. B 26 (1982) 4111.
[37] D.J. Darensbourg, B.L. Mueller, J. Bischoff, S.S. Chojnacki, J.H. Reibenspies, Inorg. Chem. 30 (1991) 2418.